Catal Lett (2008) 122:111–114
DOI 10.1007/s10562-007-9354-8

Preparation of Low Loading Pt/C Catalyst by Carbon Xerogel Method for Ethanol Electrooxidation

**Dong-Yun Zhang · Zi-Feng Ma · Guoxiu Wang ·
Jun Chen · Gorden C. Wallace · Hua-Kun Liu**

Received: 23 June 2007 / Accepted: 13 November 2007 /

Abstract Low platium loading Pt/C catalyst was prepared by direct Pt-embedded carbon xerogel method. The Pt content of the as-prepared Pt/C is about 4.32 wt% and has a typical polycrystalline phase. Textural and structural characteristics of the catalysts were characterized by XRD, EDS and BET. Pt-embedded in carbon xerogel increases the specific surface area and pore volume of the X-Pt/C during carbon gelation and the carbonization process. Electrochemical characteristics of the catalysts for ethanol electrooxidation were measured. The results indicated that the as-prepared 4.32 wt% Pt/C has higher mass current density in ethanol electrooxidation as compared to the 20 wt% Pt/C. This may be due to the high roughness of the Pt surface that is formed during the carbon gelation and carbonization process.

Keywords Pt/C catalyst · Carbon xerogel · Ethanol electrooxidation · Fuel cell

1 Introduction

In PEMFC and DMFC, the anodic oxidation of combustibles and the cathodic reduction of oxygen should be catalyzed to occur at adequate rates at low temperatures [1]. Carbon-supported platinum or platinum-based nanoparticles are the best catalysts for anodic and cathodic reactions. These catalysts are produced mainly by impregnation [2], precipitation and colloid methods [3]. The conventional preparation techniques based on impregnation and precipitation often do not provide adequate control of the shape and size of particles [4]. The colloidal methods based on microemulsions [5], sonochemistry [6], and the alcohol-reduction process [7] are, in principle, more conducive to generate colloids and clusters on the nanoscale with good uniformity. Surfactants have been widely used as stabilizers to prevent metal colloids from forming agglomerates during the reduction process in all the colloid methods. However, the residual surfactant shell on the metal particles, which blocks the catalytic reaction on the metal surface, is difficult to remove. Alternative routes based on microwave irradiation have been developed [8, 9], with good results even in the absence of surfactants. A new fabrication method for producing carbon-supported platium or platinum based catalysts directly by Pt-embedded silica or anodic aluminum oxide (AAO) membrane templates has been reported by Zhang [10] and Kim [11] recently. It provides a time saving route for the preparation of carbon-supported platinum catalysts without an additional Pt impregnation step. Although template methods provide a highly ordered porous structure, it is complex to produce Pt-embedded templates.

The carbon xerogel method, which produces porous carbon from resorcinol-formaldehyde resins, has been

---

D.-Y. Zhang · Z.-F. Ma (✉)
Department of Chemical Engineering,
Shanghai Jiaotong University, Shanghai 200240, P.R. China
e-mail: zfma@sjtu.edu.cn

G. Wang · J. Chen · G. C. Wallace · H.-K. Liu
ARC Centre of Excellence for Electromaterials Science,
University of Wollongong, Wollongong, NSW 2522, Australia

G. Wang · H.-K. Liu
ISEM, University of Wollongong, Wollongong, NSW 2522,
Australia

thoroughly studied by Job et al. [12, 13]. The pore size and specific surface area of the porous carbon can be controlled by adjusting the precursors, the gelation conditions, and the metal catalysts. The products of the carbon xerogel method are dried by simple evaporation. In this letter, low Pt loading catalyst has been directly prepared by the carbon xerogel method. The electrochemical characteristics of ethanol electrooxidation have been measured.

2 Experimental

The Pt/carbon xerogel catalyst was prepared as follows: A equimolar solution of H_2PtCl_6 (A.C.S. reagent, Sigma-Aldrich) and ethylene diaminetetra acetic acid (EDTA, Sigma-Aldrich) was added to a 0.29 M resorcinol (Sigma-Aldrich) solution and ultrasonically dispersed. Then 0.57 M formaldehyde (37.6% in methanol, Sigma-Aldrich) was added dropwise into the mixture and ultrasonically dispersed. The pH value was controlled to be in the range of 6.5–7.4 by adding 0.5 M Na_2CO_3 solution. The solution was then put into an ampoule, and sealed and heated in a drier for five days at the constant temperature of 85%. Then these samples were dried at 150% under vacuum (10^3 Pa) for three days. After drying, the gels were pyrolyzed as reported elsewhere [12]. The as-prepared catalyst was denoted as X-Pt/C, where X signifies “xerogel”.

The pore texture of the porous carbon, both with and without Pt, was characterized by the analysis of nitrogen adsorption-desorption isotherms at 77 K with a NOVA^{TM} 1000 instrument. The crystal structure of the samples was measured by X-ray diffraction (XRD) using a Philips PW1730 generator and diffractometer with Cu Kα ($\lambda = 1.54056$ Å) radiation and a graphite monochromator. Transmission electron microscopy (TEM) was carried out using a JEOL JEM 2011 analytical instrument. The particle sizes were determined both by direct measurement from bright-field electron micrographs and from the Pt (220) diffraction peak broadening using Scherrer’s formula.

Platinum content was estimated by large area standard less energy dispersive spectroscopy (EDS) using a JEOL JSM-6460 A scanning electron microscope equipped with the JEOL JED-2300 EDS analysis system. The normal Pt content in the X-Pt/C catalyst is 4.32 wt%. A 20 wt% Pt/C commercial catalyst (Johnson Matthey) was also characterized for comparison.

Electrochemical characterizations were carried out using a CHI 660 Electrochemical workstation equipped with a conventional three-electrode test cell using Pt wire as a counter electrode, saturated Hg/Hg_2SO_4 electrode as a reference electrode, and Pt/C modified glassy carbon (GC) as a working electrode. 10 μL of the catalyst ink (2 mg Pt/C catalyst in 1 mL deionized water) was cast onto the GC electrode and then dried to form a working electrode. Ethanol electrooxidation over the Pt/C modified GC electrode was investigated in an argon saturated 0.5 M C_2H_5OH/0.5 M H_2SO_4 solution. In the results, all potential values were transformed to values versus reversible hydrogen electrode (RHE).

3 Results and Discussion

Figure 1 shows the XRD patterns of the X-Pt/C and 20 wt%Pt/C catalysts. The diffraction peaks at 40, 46, 68, and 81° correspond to the Pt (111), (200), (220), and (311) planes, respectively, which represent the typical pattern of a polycrystalline Pt face-centered cubic (fcc) phase. Apart from the four diffraction peaks of platinum, another diffuse diffraction peak appears at around 21°, which could indicate the presence of amorphous carbon. The particle size obtained from the XRD pattern is 9.7 nm, in good agreement with the mean particle size of about 8.0 nm that was obtained from the TEM bright-field images (Fig. 2). Those particles which appear dark in the bright-field image correspond to Pt. The presence of the Pt nanoparticles is confirmed by the associated spotty ring in the selected area electron diffraction pattern in the insert, where the bright spots correspond to (111) and (200) Pt reflections, with additional diffuse rings correspond to amorphous carbon. Dark-field imaging (insert in Fig. 2) was also employed to confirm that the particles shown correspond to Pt. According to the BET comparison in Table 1, Pt deposition on carbon with impregnation (X-560-Pt [14]) or reductant reduction method (20 wt% Pt/C) may lead to a decrease in the specific surface area, $S_{BET.}$ Nevertheless, for X-Pt/C, the S_{BET} increases slightly as compared to the xerogel carbon; Pt-embedded in carbon xerogel increases the specific surface area and pore volume of the X-Pt/C during

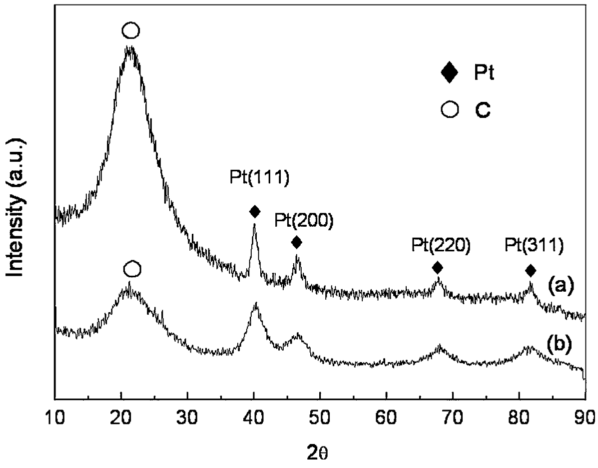

Fig. 1 XRD patterns of the (**a**) X-Pt/C and (**b**) 20 wt% Pt/C catalysts

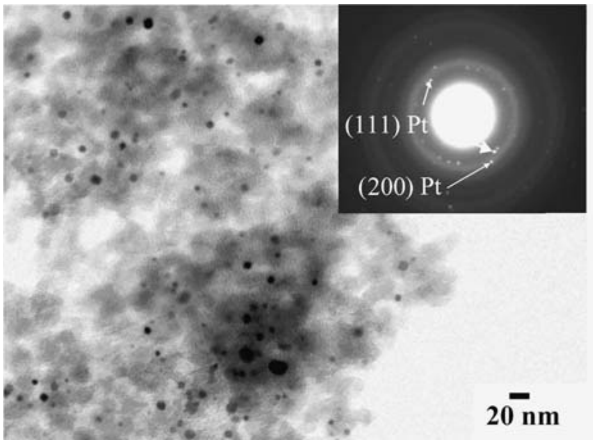

Fig. 2 TEM image of X-Pt/C catalyst. Insertion: transmission electron diffraction pattern

carbon gelation and the carbonization process. The reason for this is unclear and requires further investigation.

Figure 3 shows SEM images of xerogel carbon with/without Pt. The xerogel carbon without Pt consists of roughly rectangular particles, as shown in Fig. 3a. However, the X-Pt/C catalyst has much smaller particles, as illustrated in Fig. 3b. These micrographs demonstrate that the X-Pt/C had a much larger porous structure as compared to the xerogel carbon, and this may be useful in further catalytic applications.

Table 1 Textural characteristics of carbon supports and of Pt/C catalysts

Samples	S_{BET} (m^2/g)	$d_{p.ave}$ (nm)	$d_{p.max}$ (nm)
X-carbon	518.31	26.00	30.74
Carbon black	277.24	25.19	30.79
X-560-carbon [14]	615.00	–	40.00
X-Pt/C	562.97	25.90	30.84
20 wt% Pt/C	153.65	24.90	30.93
X-560-Pt [14]	545.00	–	40.00

S_{BET}—apparent BET surface area; $d_{p,ave}$—average pore diameter; $d_{p,max}$—maximum pore diameter

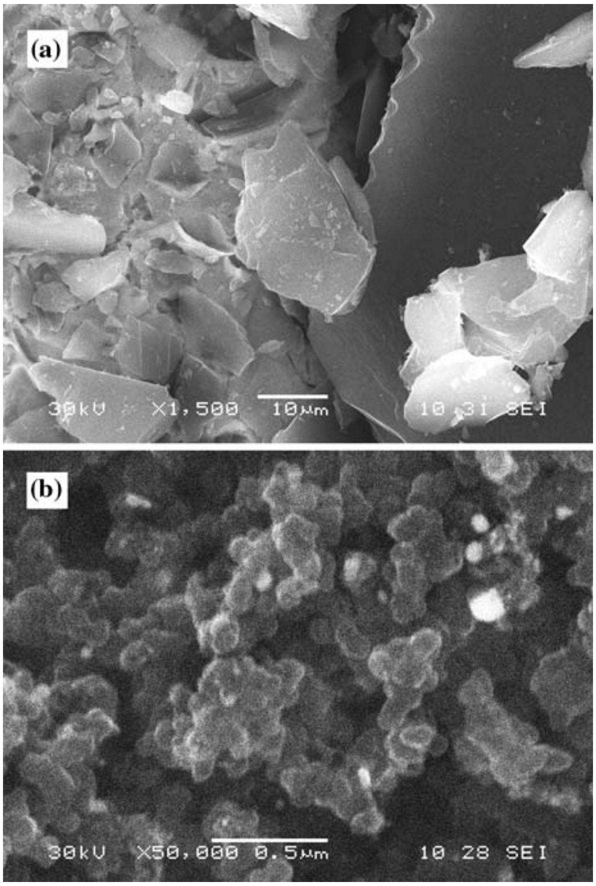

Fig. 3 SEM images of (**a**) xerogel carbon and (**b**) X-Pt/C catalyst

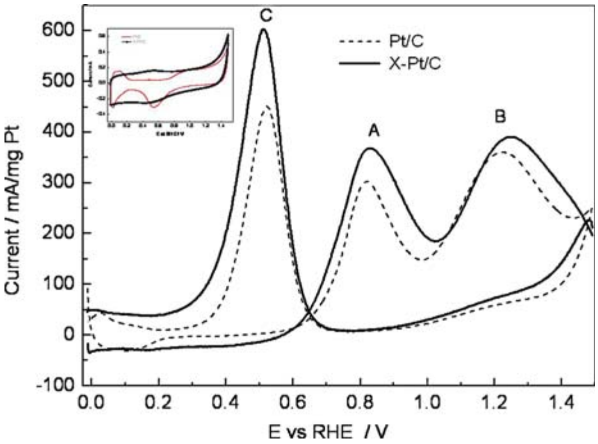

Fig. 4 Cyclic voltammograms of the X-Pt/C and 20 wt% Pt/C catalysts in 0.5 M H_2SO_4 with 0.5 M C_2H_5OH at scan rate of 50 mV/s. Insertion: reference for cyclic voltammograms with 0.5 M H_2SO_4

The electrochemical characteristics of X-Pt/C and 20 wt% Pt/C for ethanol electro-oxidation are shown in Fig. 4. The CV curves of X-Pt/C and 20 wt% Pt/C in 0.5 M H_2SO_4 solution are also inserted in Fig. 4 for reference. Two oxidation peaks (labeled as A and B), are observed during the forward sweep process for both X-Pt/C and 20 wt% Pt/C. During the backward sweep process, an anodic peak (labeled as C) is observed at around 0.50 V for X-Pt/C and 0.52 V for 20 wt% Pt/C, which is attributed to the removal of the incompletely oxidized carbonaceous species formed in the forward scan in the electrolyte [14, 15]. Here, the oxidation peak currents are nominalized mass current density, i.e. current density in mA/mg Pt. According to Fig. 4, the mass current density of the two oxidation peaks for X-Pt/C are higher than that of the 20 wt% Pt/C. X-Pt/C, with a loading of 4.32 wt%, exhibits similar catalytic activity as compared to the 20 wt% Pt/C.

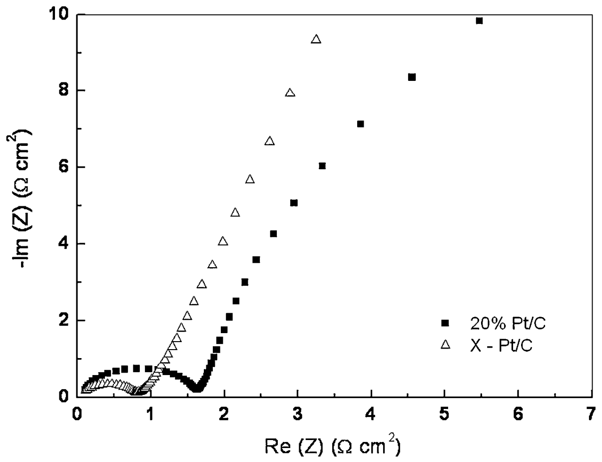

Fig. 5 AC impedance of the X-Pt/C and 20 wt% Pt/C catalysts in 0.5 M H_2SO_4 with 0.5 M C_2H_5OH at 0.6 V, frequency range: 1 Hz–100 KHz

The EIS behaviors of the catalysts are shown in Fig. 5. The diameter of the first semi circular arc of X-Pt/C is about 50% smaller than that of 20 wt% Pt/C, which indicates an ohmic process, as reported by Jens T. Mueller [16]. It may relate to electrical conduction via an electrical double layer between the X-Pt/C catalyst particle and aqueous electrolyte (as previously reported [17]), or to the decrease in contact resistance between Pt and carbon. However, the diameter of the secondary circular arc for X-Pt/C is larger than that for 20 wt% Pt/C. It means that the kinetic resistance increases with decreasing Pt loading. As previously reported [18], the low Pt loading catalysts show higher catalytic activity than high Pt loading catalysts because of their smaller particles and higher surface area. However, in this case, the mean particle size of the X-Pt/C is larger than that of 20 wt% Pt/C. Thus, the high mass electrocatalytic activity might be attributed to the high roughness of the Pt surface, which is produced during carbon gelation and carbonization.

4 Conclusions

A catalyst of 4.32 wt% Pt on carbon support is obtained by mixing Pt salt with the precursor of carbon xerogel. The as-prepared Pt/C has a typical polycrystalline phase and uniform Pt dispersion with a mean particle size around 8 nm. Comparing to the 20 wt% Pt/C, the 4.32 wt% Pt/C has much higher mass current density for ethanol electro-oxidation. The EIS behavior of the catalyst indicates the X-Pt/C has lower ohmic resistance than that of the 20 wt%Pt/C. Although the X-Pt/C catalyst has lower Pt loading and a larger Pt particle size, high mass electrocatalytic activity has been observed. The direct Pt-embedded carbon xerogel method may provide a much simpler route for producing a low loading Pt/C catalyst.

Acknowledgments The authors are grateful for the financial support of this work by the National Science Foundation of China (20476055, 20060248064), the Science & Technology Commission of Shanghai Municipality (06SN07115, 065211020), and the Sino-Australian Special Foundation of Science and Technology (20710082).

References

1. Steele BCH, Heinzel A (2001) Nature 414:345
2. Hoogers G (2003) Fuel cell technology handbook. CRC Press, Florida, Chap 6, p. 15
3. Liu ZL, Lee JY, Han M, Chen WX, Gan LM (2002) J Mater Chem 12:2453
4. Armadi IS, Wang ZL, Green TC, Henglein A, El-Sayed MA (1996) Science 272:1924
5. Rojas S, García- García FJ, Järas S, Martínez-Huerta MV, Fierro JLG, Boutonnet M (2005) Appl Catal A Gen 285:24
6. Fujimoto T, Teraushi S, Umehara H, Kojima I, Henderson W (2001) Chem Mater 13:1057
7. Spinacé EV, Neto AO, Vasconcelos TRR, Linardi M (2004) J Power Sources 137:17
8. Komarneni S, Li DS, Newalkar B, Katsuki H, Bhalla AS (2002) Langmuir 18:5959
9. Chen WX, Lee JY, Liu ZL (2002) Chem Commun 2588
10. Zhang L, Cheng B, Samulski ET (2004) Chem Phys Lett 398:505
11. Kim P, Joo JB, Kim W, Kim H, Song JY (2005) Carbon 43:2397
12. Job N, Pirard R, Marien J, Pirard J-P (2004) Carbon 42:619; 42:3217
13. Job N, Pereira MFR, Lambert S, Cabiac A, Delahay G, Colomer J-F, Marien J, Figueiredo JL, Pirard J-P (2006) Catal J 240:160
14. Manohara R, Goodenough JB (1992) J Mater Chem 2:875
15. Song SQ, Zhou WJ, Zhou ZH, Jiang LH, Sun GQ, Xin Q, Leontidis V, Kontou S, Tsiakaras P (2005) Int J Hydrogen Energ 30:995
16. JT Mueller PM Urban (1998) J Power Sources 75:139
17. Otomo J, Li X, Kobayashi T, Ching-ju W, Hidetoshi N, Takahashi H (2004) J Electroanal Chem 573:99
18. Ticianelli EA, Derouin CR, Srinivasan S, Electroanal J (1988) Chem 251:275